To appear in The Astronomical Journal, January 2006 issue

# The Astrometric-Spectroscopic Binary System HIP 50796: An Overmassive Companion

Guillermo Torres

*Harvard-Smithsonian Center for Astrophysics, 60 Garden St., Cambridge, MA 02138*

gtorres@cfa.harvard.edu

## ABSTRACT

We report spectroscopic observations of the star HIP 50796, previously considered (but later rejected) as a candidate member of the TW Hya association. Our measurements reveal it to be a single-lined binary with an orbital period of 570 days and an eccentricity of $e = 0.61$. The astrometric signature of this orbit was previously detected by the HIPPARCOS satellite in the form of curvature in the proper motion components, although the period was unknown at the time. By combining our radial velocity measurements with the HIPPARCOS intermediate data (abscissae residuals) we are able to derive the full three-dimensional orbit, and determine the dynamical mass of the unseen companion as well as a revised trigonometric parallax that accounts for the orbital motion. Given our primary mass estimate of 0.73 $M_\odot$ (mid-K dwarf), the companion mass is determined to be 0.89 $M_\odot$, or $\sim$20% *larger* than the primary. The likely explanation for the larger mass without any apparent contribution to the light is that the companion is itself a closer binary composed of M dwarfs. The near-infrared excess and X-ray emission displayed by HIP 50796 support this. Our photometric modeling of the excess leads to a lower limit to the mass ratio of the close binary of $q \sim 0.8$, and individual masses of 0.44—0.48 $M_\odot$ and 0.41—0.44 $M_\odot$. The new parallax ($\pi = 20.6 \pm 1.9$ mas) is significantly smaller than the original HIPPARCOS value, and more precise.

*Subject headings:* binaries: spectroscopic — binaries: visual — stars: individual (HIP 50796) — stars: late-type — techniques: radial velocities — techniques: spectroscopic

## 1. Introduction

In recent years there has been considerable interest in the study of nearby groupings of young stars that do not appear to be associated with any molecular clouds. The prototypical example is perhaps the TW Hydrae association (Kastner et al. 1997), with an estimated age of 8–10 Myr and some two dozen members. Searches for new members of this group have relied on X-ray properties, kinematics, infrared (2MASS) colors, and spectral features (e.g., Makarov & Fabricius 2001; Gizis 2002; Tachihara et al. 2003; Song, Zuckerman & Bessell 2003), and have produced many candidates and motivated detailed follow-up studies to confirm them.

One of those searches, by Makarov & Fabricius (2001), used proper motions from the Tycho-2 catalog (Høg et al. 2000) for X-ray sources listed in the ROSAT Bright Source Catalog (Voges et al. 1999). The authors considered a large area surrounding the previously known members of the TW Hya association, and proposed a list of 23 candidate members that were subsequently followed up spectroscopically by Torres, Neuhäuser & Latham (2001), Song, Bessell & Zuckerman (2002), and Torres et al. (2003). The present paper discusses one of those objects, HIP 50796 (also known as BD−09 3055, GSC 05493 00324, 1RXS J102219.2−103302, TYC 5493–324–1, $\alpha = 10^{\rm h}22^{\rm m}17\overset{\rm s}{.}99$, $\delta = -10^\circ 32' 15\overset{''}{.}5$, J2000, $V = 10.80$, SpT = K). The kinematic model of the association constructed by Makarov & Fabricius (2001) made specific predictions as to the radial velocity expected for each candidate. Although the measurements for HIP 50796 by Torres, Neuhäuser & Latham (2001) happened to agree perfectly with those predictions ($+13.1 \pm 1.0$ km s$^{-1}$), Song, Bessell & Zuckerman (2002) found that the star shows no detectable Li $\lambda$6708 absorption in its spectrum (equivalent width $< 10$ mÅ), which indicates it is not very young and therefore essentially rules it out as a true member. They also measured a radial velocity of $+22.4 \pm 0.9$ km s$^{-1}$ that is nearly 10 km s$^{-1}$ different from the previous measurements, and proposed that the object is a spectroscopic binary. Further measurements by Torres et al. (2003) confirmed the velocity variations and indicated an orbital period of perhaps 1 or 2 years.

Even though it was clear that HIP 50796 is not related the TW Hya association, the object was kept on the observing list at the Harvard-Smithsonian Center for Astrophysics (CfA) for the purpose of establishing the orbit. Preliminary solutions appeared to imply a mass for the companion that is larger than the primary, which was puzzling given that the spectrum is single-lined. Additionally, the HIPPARCOS satellite (ESA 1997) detected curvature in the proper motion further supporting the binary nature of the object. We present here the complete analysis of HIP 50796 that combines the astrometry and the spectroscopy and allows us to investigate in more detail the nature of the overmassive secondary star.

## 2. Spectroscopic observations and reductions

HIP 50796 was observed spectroscopically at the CfA with an echelle spectrograph on the 1.5-m Tillinghast reflector at the F. L. Whipple observatory on Mt. Hopkins (Arizona). A single echelle order was recorded using a photon-counting intensified Reticon detector at a central wavelength of 5187 Å, giving a spectral coverage of 45 Å. The resolving power is $\lambda/\Delta\lambda \approx 35{,}000$. A total of 34 spectra were obtained from April 2002 until May 2005, and the signal-to-noise (S/N) ratios achieved range from 5 to about 30 per resolution element of 8.5 $\mathrm{km\,s^{-1}}$. Four archival spectra (S/N of 9–30) were also used, and were obtained for another program in 1985–1986 with nearly identical instrumentation on the Multiple Mirror Telescope (also on Mt. Hopkins, Arizona), prior to its conversion to a monolithic mirror.

Radial velocities were derived using `XCSAO` (Kurtz & Mink 1998), a one-dimensional cross-correlation program well suited to our relatively low S/N spectra that runs under IRAF[1]. For the template we used a synthetic spectrum selected from an extensive library of spectra based on model atmospheres by R. L. Kurucz[2] (see Nordström et al. 1994; Latham et al. 2002). These calculated spectra are available for a wide range of effective temperatures ($T_{\rm eff}$), projected rotational velocities ($v \sin i$), surface gravities ($\log g$) and metallicities. The optimum template was determined from grids of cross-correlations over broad ranges in $T_{\rm eff}$ and $v \sin i$, seeking to maximize the average correlation weighted by the strength of each exposure. Solar metallicity was assumed to begin with. The above calculations were repeated for a range of $\log g$ values from 2.0 to 5.0, which allowed us to derive a rough estimate of the surface gravity for HIP 50796. We obtained $\log g = 4.2 \pm 0.5$ and $T_{\rm eff} = 4600 \pm 150$ K. The entire procedure was repeated for metallicities different from solar, but the best match was achieved for templates with the solar composition. The temperature we derive corresponds to a main-sequence star with spectral type mid-K (Cox 2000). The rotational broadening was found to be negligible (formally $v \sin i = 1 \pm 3$ $\mathrm{km\,s^{-1}}$). Song, Zuckerman & Bessell (2003) reported a considerably larger value of 8 $\mathrm{km\,s^{-1}}$.

The stability of the zero-point of our velocity system was monitored by means of exposures of the dusk and dawn sky, and small run-to-run corrections were applied in the manner described by Latham (1992). The radial velocities in the heliocentric frame including these corrections are listed in Table 1. The typical precision of a single measurement is 0.5 $\mathrm{km\,s^{-1}}$. Variations over the 19.4 years of coverage are obvious and show a peak-to-peak amplitude of about 40 $\mathrm{km\,s^{-1}}$. The period is 570 days, and the eccentricity ($e = 0.61$) is quite significant.

---

[1]IRAF is distributed by the National Optical Astronomy Observatories, which is operated by the Association of Universities for Research in Astronomy, Inc., under contract with the National Science Foundation.

[2]Available at `http://cfaku5.cfa.harvard.edu`.

An orbital solution based on these velocities is presented in the second column of Table 2. Although it is no longer relevant in connection with the possible membership to the TW Hya association, we mention in passing that the center-of-mass velocity $\gamma = +24.77 \pm 0.14$ km s$^{-1}$ of HIP 50796 is far from the value of +13.1 km s$^{-1}$ that had been predicted by Makarov & Fabricius (2001). The most significant finding, however, is the large mass function of the binary: $f(M) = 0.258 \pm 0.011$. For a typical primary mass corresponding to the temperature we derive, the mass function implies a secondary that is more massive than the primary, yet no signs of another star are obvious in our spectra. We discuss this further below.

## 3. Astrometric observations

HIP 50796 was observed by the HIPPARCOS satellite from December 1989 to November 1992, during which 53 astrometric measurements were made. The trigonometric parallax was determined to be $\pi_{\rm HIP} = 29.40 \pm 2.69$ mas. The uncertainty is somewhat larger than usual, but perhaps understandably so given that the star is relatively faint ($V = 10.80$). Additionally, the HIPPARCOS reductions revealed significant curvature in the proper motion in the amount of $d\mu_\alpha/dt = -10.90 \pm 6.51$ mas yr$^{-2}$ and $d\mu_\delta/dt = +22.33 \pm 5.84$ mas yr$^{-2}$, most likely a reflection of the orbital motion of the object. Given its period of 570 days, however, nearly two cycles of the orbit were covered during the HIPPARCOS campaign (which lasted 1058 days) so that the meaning of those coefficients is obscured. The proper motions and the parallax as reported in the HIPPARCOS catalog are also likely to be compromised.

Since the satellite observations are sensitive enough to have detected the orbital motion on the plane of the sky, the best course of action is therefore to make use of the individual astrometric measurements ("abscissae residuals"; ESA 1997) together with the velocities to constrain the orbit, and at the same time re-derive the position, proper motion, and parallax. Those HIPPARCOS measurements are listed in Table 3. We describe the global solution below.

## 4. Orbital solution

The radial velocities allow for the determination of the usual spectroscopic elements, which are the period ($P$), center-of-mass velocity ($\gamma$), semi-amplitude of the velocity variation ($K$), eccentricity ($e$), longitude of periastron for the primary ($\omega_1$), and time of periastron passage ($T$). On the other hand, the visual elements constrained by the astrometry are the angular semimajor axis ($a$), the inclination angle ($i$), the position angle of the ascending

node ($\Omega$), as well as $P$, $e$, $\omega_1$, and $T$. The combination of the two kinds of measurements thus provides redundancy in the four latter orbital elements that strengthens the solution. Furthermore, the fact that we see no indication of the secondary in the spectrum of HIP 50796 means that the motion seen by HIPPARCOS should essentially be that of the primary star around the center of mass of the binary. This introduces a relation between the angular semimajor axis of the primary, $a_1$, and its velocity amplitude, given by

$$a_1 = 9.191967 \times 10^{-5} \cdot \pi K P \sqrt{1-e^2} / \sin i \ , \tag{1}$$

where $a_1$ and the trigonometric parallax $\pi$ are expressed in milli-arc seconds, $K$ in $\mathrm{km\,s^{-1}}$, and $P$ in days. We use this relation to eliminate the angular semimajor axis ($a_1$) as an unknown. Since the HIPPARCOS observations are made in an absolute frame of reference, the abscissae residuals contain information on the parallax as well as the position and proper motion of the barycenter of the binary. Five additional variables are thus introduced ($\Delta\alpha^*$, $\Delta\delta$, $\Delta\mu_\alpha^*$, $\Delta\mu_\delta$, $\Delta\pi$)[3], which represent corrections to a fiducial point of reference that yield improved estimates of those quantities over the catalog values (see ESA 1997).

A total of 13 variables were adjusted in the solution, using standard non-linear least-squares techniques (Press et al. 1992). The formalism used for incorporating the abscissae residuals from HIPPARCOS into the fit follows closely that described by van Leeuwen & Evans (1998) and Pourbaix & Jorissen (2000), and is described in more detail in the Appendix. The relative weights of the spectroscopic and astrometric observations were adjusted to yield separate reduced $\chi^2$ values near unity. In this way we determined a scale factor for the original uncertainties of the HIPPARCOS abscissae residuals of 1.14, and a factor of 1.43 for the original velocity errors.

Due to the faintness of the target the median error of a single HIPPARCOS measurement is 5.7 mas, so that the constraint provided by the astrometry is relatively weak. Nevertheless, the results of this initial fit yielded improvements in all of the orbital elements in common with the spectroscopy. The value derived for the angular semimajor axis of the primary was $a_1 = 16.9 \pm 1.6$ mas. As a test to see if the astrometry is able to detect the light contribution from the companion, we ran another solution in which we left the semimajor axis of the apparent orbit as a free parameter. In this case that semimajor axis ($a_{\rm phot}$) corresponds to the motion of the center of light of the binary, or photocenter, rather than that of the primary, and it should in principle be smaller if the light from the secondary is significant. This fit gave a value of $a_{\rm phot} = 18.1 \pm 3.6$ mas, which is not only not smaller but is also much more uncertain (because it is no longer constrained by the spectroscopy through eq.[1]).

[3]Following the practice of the HIPPARCOS catalog we define $\Delta\alpha^* \equiv \Delta\alpha \cos\delta$ and $\Delta\mu_\alpha^* \equiv \Delta\mu_\alpha \cos\delta$.

Nevertheless, it is still consistent with the previous result, within the errors. We conclude from this that the companion is not bright enough to produce a measurable astrometric effect, and we proceed under the assumption that that star is invisible (but see §6).

Slight differences were found in the proper motion components ($\mu_\alpha^*$, $\mu_\delta$) compared to the values reported in the HIPPARCOS catalog, which was not unexpected given that the catalog values do not account for orbital motion. An external check on these motions is available from the Tycho-2 catalog (Høg et al. 2000), in which $\mu_\alpha^*$ and $\mu_\delta$ are derived by combining the HIPPARCOS position (mean epoch 1991.25) with positions from ground-based meridian-circle and photographic catalogs going back several decades, and up to a century in some cases. Given that the period of HIP 50796 is only 570 days, the orbital motion over a baseline of decades should tend to average out in the Tycho-2 analysis, resulting in a more accurate measure of the proper motion than that reported by HIPPARCOS. Indeed, as shown in Table 4 the values of $\mu_\alpha^*$ and $\mu_\delta$ from our initial fit are much closer to the Tycho-2 values than the HIPPARCOS values. This also suggests that the solution might benefit if we made use of the constraint provided by Tycho-2. Consequently, we incorporated the Tycho-2 proper motions into the fit as measurements, along with their uncertainties. The resulting proper motions from this combined solution are listed for comparison in the fourth row of Table 4. The remaining orbital elements are hardly affected, except for the slightly smaller uncertainties.

The complete results of this combined fit are given in the third column of Table 2. The semimajor axis of the relative orbit, $a$, is inferred to be 30.8 mas (1.58 AU in linear units). The orbital period is determined to better than 0.1% by virtue of the 19.4-yr baseline provided by the velocity measurements (more than 12 cycles). Perhaps one of the most significant improvements coming from the combination of the astrometry and spectroscopy is in the trigonometric parallax. Compared to the value from the HIPPARCOS catalog, our parallax that takes full account of the orbital motion is nearly 10 mas smaller, which corresponds to a 50% change in the distance to HIP 50796 (see Table 4), and is considerably more precise. This has important consequences for the luminosity estimates discussed below.

According to our solution the orbit of the binary is seen nearly edge-on: the inclination angle is $85^\circ \pm 13^\circ$. Although in principle this would allow for eclipses, these are very unlikely given the 570-day period. Inspection of the HIPPARCOS photometry for HIP 50796 shows no evidence of any eclipse events (four conjunctions occurred during the mission), and the peak-to-peak brightness variation recorded is $\sim$0.1 mag, which is probably at the level of the uncertainties for a star as faint as $V = 10.80$. Nevertheless, carefully scheduled observations may perhaps be of interest since the satellite measurements do not have the optimal sampling.

## 5. The nature of the companion

The information provided by our combined solution allows a direct determination of the mass of the unseen companion of HIP 50796, given an estimate of the primary mass. For this we use our effective temperature determination in §2 ($T_{\rm eff} = 4600 \pm 150$ K), and the brightness of the object. The latter was measured during the HIPPARCOS mission as $H_p = 10.9366 \pm 0.0055$, in the passband of the satellite. Conversion to the Johnson system (ESA 1997) yields $V = 10.80 \pm 0.02$, where the uncertainty is our conservative estimate that includes the transformation. With our parallax of $\pi = 19.5 \pm 1.8$ mas (corresponding to a distance of $51.3 \pm 4.9$ pc) the absolute magnitude in the visual band is $M_V = 7.25 \pm 0.20$, ignoring extinction, in which essentially all of the uncertainty comes from the parallax error.

The location of the primary star in the H-R diagram is shown in Figure 1. Model isochrones from the series by Girardi et al. (2000) for solar metallicity agree well with the measured properties of HIP 50796, quite independently of age (ranging from 1 Gyr to 5 Gyr in the figure). From these models we estimate the primary mass to be $M_1 = 0.73 \pm 0.05$ $M_\odot$, in which the uncertainty accounts for observational errors as well as age. The surface gravity inferred from the models is $\log g = 4.65 \pm 0.05$, in agreement with our crude estimate from §2. Although the precise metallicity of the star is unknown, our tests in §2 suggested a composition near solar. Additionally, the space motion of HIP 50796 in the Galactic frame based on our parallax, proper motion, and center-of-mass velocity is quite small ($U = -8$ km s$^{-1}$, $V = -14$ km s$^{-1}$, $W = +9$ km s$^{-1}$, relative to the Local Standard of Rest), which supports a Population I origin and a heavy element abundance probably close to that of the Sun, as we have assumed.

The adopted mass for the primary leads to a companion mass of $M_{\rm comp} = 0.88 \pm 0.05$ $M_\odot$. The uncertainty in the primary mass contributes only about 25% to this error. The secondary star is thus 20% more massive than the primary, which implies it cannot be a single main-sequence star. A more careful examination of our spectra was carried out using the two-dimensional cross-correlation algorithm TODCOR (Zucker & Mazeh 1994), to place limits on the brightness of the companion. This technique often allows the detection and measurement of faint secondaries that are difficult to see in standard one-dimensional cross-correlation diagrams. No evidence of another set of lines was found down to the level of the noise, at about 10% of the brightness of the primary. Additionally, Hemenway et al. (1997) reported an observation of HIP 50796 by speckle interferometry in which no companions were apparently seen in the range from 30 mas to $0\farcs7$. Details of this measurement are unavailable.

One possibility is that the companion is a white dwarf. Depending on its temperature, it may be possible to detect it in the ultraviolet, although no such observations are available to our knowledge. Given the present mass of the object, initial-final mass relations for white

dwarfs (e.g., Ferrario et al. 2005, and references therein) suggest a progenitor of approximately 4–5 $M_\odot$, corresponding to a mid-B star. Alternatively, the companion of HIP 50796 could itself be a (closer) binary composed of lower main-sequence stars, making the system a hierarchical triple. In this case, however, the mass ratio of the binary cannot be too small or we would have seen the brighter of the two stars in our spectra[4].

Possible signs of this type of configuration might be seen in the form of an infrared excess. $JHK_s$ measurements for HIP 50796 are available from the 2MASS catalog. With the visual magnitude listed earlier, and after conversion to the standard Johnson system as defined by Bessell & Brett (1988) using transformations by Carpenter (2001), we obtain the observed colors $V-J$, $V-H$, and $V-K$ listed in the first line of Table 5. The predicted colors for a single star of the assumed mass ($M_1 = 0.73$ $M_\odot$) according to the models by Girardi et al. (2000) for a representative age of 2 Gyr are indeed bluer, by as much as 0.4 mag. However, there are a number of reasons to doubt the theoretical colors in this case, including indications of missing opacity sources and other limitations in the physics (e.g., Baraffe et al. 1998; Delfosse et al. 2000; Chabrier et al. 2005, and references therein), and especially disagreements with empirical mass-luminosity relations, particularly in the visual band. Therefore, we have chosen here to rely on the empirical relations. Those by Henry & McCarthy (1993) give redder colors than Girardi et al. (2000) for the primary (see third line of Table 5), but are still considerably bluer than observed, by 0.17 mag, 0.29 mag, and 0.25 mag for $V-J$, $V-H$, and $V-K$, respectively. These differences are 6–7 times larger than the observational errors, suggesting the infrared excess may be real.

With the aid of the Henry & McCarthy (1993) relations, we have modeled this excess by computing the visual and $JHK$ magnitudes of the components of the unseen companion (hereafter star 2 and star 3) over a range of possible masses for each star, subject to the constraint that their sum be the value we determined above, $M_{\rm comp} = 0.88$ $M_\odot$. We then added the light of these stars to that of the primary (star 1) in each passband, and calculated the combined colors for the triple system. For convenience we parameterized the problem in terms of the mass ratio of the binary ($q = M_3/M_2$, where star 2 is the more massive component). Additionally, we allowed for changes in the mass of the main star, and sought to produce the best match to the observed colors as well as the combined absolute visual magnitude, in a $\chi^2$ sense. A solution was found for a mass $M_1 = 0.728$ $M_\odot$ and a binary mass ratio $q = 0.795$, which reproduces the observed visual brightness and all infrared colors within the uncertainties (see last row of Table 5). Contours of the $\chi^2$ surface as a function of

[4]A possible exception would be if the orbital period of the binary is short enough that the stars are spun up by tidal forces and are rotating very rapidly, in synchronism with the orbital motion. In that case the spectral lines may be broad enough to reduce the contrast and escape detection.

$M_1$ and $q$ are shown in Figure 2, where the best fit is indicated by a dot. The masses of the binary components from this model are $M_2 = 0.49$ $M_\odot$ and $M_3 = 0.39$ $M_\odot$. The predicted magnitude difference in the visual band between the brighter of these stars and star 1 is 3.0 mag, which is below our threshold for spectroscopic detection ($\sim$2.5 mag; see above) and is thus consistent with all observational constraints. Although this is formally the best fit to the observations, we note that the $\chi^2$ surface is nearly flat in the $q$ direction for $q$ larger than about 0.7–0.8 at a fixed value of $M_1$, so that larger mass ratios up to and including unity are equally acceptable and reproduce the observed colors just as well (see Figure 2). The mass of star 1, on the other hand, is very tightly constrained. At $q = 1$ stars 2 and 3 would be at their faintest, each about 3.3 mag fainter than star 1.

## 6. Constrained orbital solution

Even though, according to the model above, both stars in the binary are too faint to be seen individually in our spectra, their combined light is not negligible compared to the brightness of star 1. The difference is approximately 2.5 mag in the visual band. This suggests that our earlier assumption that the astrometric motion detected by HIPPARCOS traces only the motion of star 1 may not be entirely correct. The extra light (even with $\Delta V = 2.5$) must affect the astrometry at some level, despite our failure to detect the effect directly, as described in §4. This will cause the semimajor axis of the photocenter, $a_{\rm phot}$, to be slightly smaller than that of the primary alone by a factor $(B - \beta)/B \approx 0.17$, where $B = M_{\rm comp}/(M_1 + M_{\rm comp})$ is the mass fraction of the companion and $\beta = (1 + 10^{0.4\Delta V})^{-1}$ is its fractional light. We therefore adjusted our orbital solution to allow for this effect, and recomputed all orbital elements. The results of this "constrained" solution are seen in the last column of Table 2. The semimajor axis of the photocenter is reduced from $a_{\rm phot} = a_1 = 16.9 \pm 1.5$ mas to $a_{\rm phot} = 14.9 \pm 1.3$ mas, a small effect.

The residuals of the radial-velocity observations from this fit are listed in Table 1, and those of the HIPPARCOS measurements are given in Table 3. Figure 3 displays the spectroscopic measurements along with the velocity curve as a function of orbital phase. The astrometric observations on the plane of the sky are illustrated in Figure 4 and Figure 5, in which the axes are parallel to the Right Ascension and Declination directions. The curious pattern in Figure 4 is the result of the combined effects of annual parallax, proper motion, and orbital motion. The dominant contribution is from the proper motion (80 mas yr$^{-1}$), which is indicated with an arrow. Parallax and orbital motion are smaller and comparable effects. In Figure 5 we have subtracted the proper motion and parallactic contributions, leaving only the orbital motion with the 570-day period and a semimajor axis of $a_{\rm phot} = 14.9$ mas. The

direction of motion is direct (counterclockwise). The individual HIPPARCOS observations are represented schematically in both of these figures, but are seen more clearly in Figure 5. Because they are one-dimensional in nature (ESA 1997), the exact location of each measurement on the plane of the sky cannot be shown graphically. The filled circles represent the predicted location on the computed orbit. The dotted lines connecting to each filled circle indicate the scanning direction of the HIPPARCOS satellite for each measurement, and show which side of the orbit the residual is on. The short line segments at the end of and perpendicular to the dotted lines indicate the direction along which the actual observation lies, although the precise location is undetermined. Occasionally more than one measurement was taken along the same scanning direction, in which case two or more short line segments appear on the same dotted lines.

Compared to our previous solution, the parallax is increased slightly to $\pi = 20.6 \pm 1.9$ mas, which corresponds to a distance of $48.5 \pm 4.5$ pc. The proper motion components change very little (Table 4). The binary mass derived with $M_1 = 0.73$ $M_\odot$ is marginally larger than before ($M_{\rm comp} = 0.89 \pm 0.06$ $M_\odot$). The change in the parallax leads to a revised absolute magnitude for the system of $M_V = 7.37 \pm 0.20$. With these updated values of $M_{\rm comp}$ and $M_V$ we repeated the photometric modeling using the Henry & McCarthy (1993) mass-luminosity relations, and obtained a solution not very different from the previous one (the same value of $M_1$, and $q = 0.842$, implying $M_2 = 0.48$ $M_\odot$ and $M_3 = 0.41$ $M_\odot$). The brightness difference between star 1 and the sum of stars 2 and 3 is unchanged, making another iteration of our orbital solution unnecessary.

## 7. Discussion and concluding remarks

HIP 50796 is an interesting illustration of the complementarity of spectroscopic and astrometric observations, and in particular of the utility of the HIPPARCOS intermediate data (see also Pourbaix 2004; Jorissen, Jancart & Pourbaix 2004; Pourbaix, Jancart & Jorissen 2004). While the radial-velocity measurements clearly reveal this object to be a binary and provide the (single-lined) spectroscopic orbit with a period of 570 days, the combination with the astrometry has allowed us to derive the dynamical mass of the companion ($M_{\rm comp} = 0.89$ $M_\odot$) and also to correct the seriously biased parallax value from the original HIPPARCOS reductions. No indications of the companion are detected in our spectra, yet the orbital solution shows that it is clearly more massive than the visible star, which is a normal K dwarf with $M \approx 0.73$ $M_\odot$. While we cannot completely rule out that the secondary is a massive white dwarf, all the evidence points quite convincingly toward the conclusion that the companion is itself a closer binary composed of M dwarfs, making the system a

hierarchical triple.

The infrared excess that might be expected from such a configuration appears indeed to be present, as indicated by our modeling of the measured visual and near-infrared (2MASS) photometry using empirical mass-luminosity relations by Henry & McCarthy (1993), along with the constraint on the total mass of the unseen companion. This modeling cannot determine the precise mass ratio of the close binary, but is able to place a lower limit of about $q \approx 0.8$. Smaller values would make one of the stars bright enough that it would be seen in our spectra. We infer masses for these stars of approximately $M_2 = 0.44—0.48$ $M_\odot$ and $M_3 = 0.41—0.44$ $M_\odot$. The period of the close binary is unknown. We note also that HIP 50796 is listed as an X-ray source in the ROSAT catalog, with $\log L_X = 28.62$ (Micela, Favata & Sciortino 1997) and $\log(L_X/L_{\rm bol}) = -2.61$ (Makarov & Fabricius 2001). This X-ray emission might arise naturally from the presence of the M dwarfs, which are frequently active, particularly if they are in a short-period configuration so that tidal forces compel the stars to be in synchronous rotation with the orbital motion.

Finally, the relative orbit of HIP 50796 and its unseen companion has an angular semi-major axis of about 33 mas. Given the eccentricity of the orbit, separations up to about 50 mas are possible at times, which may permit a direct detection of the secondary with high-resolution techniques. Alternatively, infrared spectroscopy should be able to reveal the presence of at least the brighter of the M dwarfs directly, given the more favorable contrast with the main star at those wavelengths.

The author is grateful to P. Berlind, M. Calkins, D. W. Latham, and R. P. Stefanik for obtaining the spectroscopic observations used in this work, and to R. J. Davis for maintaining the CfA echelle database. B. Mason and P. Hemenway are thanked for information on speckle measurements. This paper benefited also from helpful comments by an anonymous referee. Partial support for this work from NSF grant AST-0406183 and NASA's MASSIF SIM Key Project (BLF57-04) is acknowledged. This research has made use of the SIMBAD database, operated at CDS, Strasbourg, France, of NASA's Astrophysics Data System Abstract Service, and of data products from the Two Micron All Sky Survey, which is a joint project of the University of Massachusetts and the Infrared Processing and Analysis Center/California Institute of Technology, funded by NASA and the NSF.

## A. Incorporating HIPPARCOS data into the global orbital solution

The intermediate data provided with the HIPPARCOS catalog are the "abscissae residuals", $\Delta v$, which are the difference between the satellite measurements (abscissae) along great

circles and the abscissae computed from the 5 standard astrometric parameters. The standard parameters are the position of the object ($\alpha_0^*$, $\delta_0$) at the reference epoch $t_0 = 1991.25$, the proper motion components ($\mu_\alpha^*$, $\mu_\delta$), and the parallax ($\pi$). We follow here the notation in the HIPPARCOS catalog and define $\alpha_0^* \equiv \alpha_0 \cos\delta$ and $\mu_\alpha^* \equiv \mu_\alpha \cos\delta$, to incorporate the projection factors. The goal of an orbital solution making use of the HIPPARCOS data is to reduce the abscissae residuals below the values obtained from the 5-parameter solution by taking the orbital motion into account[5]. Following Pourbaix & Jorissen (2000) the $\chi^2$ sum for the abscissae residuals is $\chi^2 = \boldsymbol{\Xi^t}\ \boldsymbol{V^{-1}}\ \boldsymbol{\Xi}$, where

$$\boldsymbol{\Xi} = \boldsymbol{\Delta v} - \sum_{k=1}^{M} \frac{\partial \boldsymbol{v}}{\partial p_k} \Delta p_k \tag{A1}$$

and $\boldsymbol{\Xi^t}$ is the transpose of $\boldsymbol{\Xi}$. In this expression $\boldsymbol{\Delta v}$ is the array of N abscissae residuals provided by HIPPARCOS, and $\partial \boldsymbol{v}/\partial p_k$ is the array of partial derivatives of the abscissae with respect to the $k$-th fitted parameter. The number $M$ of parameters fitted to the astrometry in the general case is 12: the 5 standard HIPPARCOS parameters ($p_1 = \alpha_0^*$, $p_2 = \delta_0$, $p_3 = \mu_\alpha^*$, $p_4 = \mu_\delta$, $p_5 = \pi$) and 7 orbital elements ($a_1$, $P$, $e$, $i$, $\omega_1$, $\Omega$, $T$, represented as $p_k$ with $k = 6, ..., 12$). $\boldsymbol{V^{-1}}$ is the inverse of the covariance matrix of the observations, containing the abscissae uncertainties and correlation coefficients (ESA 1997, Vol. 3, eqs. 17-10 and 17-11) also provided with the HIPPARCOS catalog. Correlations arise because the same original data were reduced independently by two data reduction consortia (NDAC and FAST; see ESA 1997), and both results are included in the solution.

The partial derivatives $\partial \boldsymbol{v}/\partial p_k$ for $k = 1$ to 5 are given in the HIPPARCOS catalog along with the abscissae residuals. The remaining derivatives can be expressed in terms of the partial derivatives of $\boldsymbol{v}$ with respect to $\alpha_0^*$ and $\delta_0$. These are (ESA 1997, Vol. 3, eq. 17-15)

$$\frac{\partial \boldsymbol{v}}{\partial p_k} = \frac{\partial \boldsymbol{v}}{\partial \alpha_0^*}\frac{\partial \xi}{\partial p_k} + \frac{\partial \boldsymbol{v}}{\partial \delta_0}\frac{\partial \eta}{\partial p_k} \quad , \quad k = 6, ..., 12, \tag{A2}$$

in which $\xi$ and $\eta$ are in our case the rectangular coordinates of the photocenter relative to the center of mass of the binary on the plane tangent to the sky at ($\alpha_0^*$, $\delta_0$), which are given by

$$\xi = \alpha_0^* + \mu_\alpha^*(t - t_0) + \pi P_\alpha + \Delta X \tag{A3}$$

$$\eta = \delta_0 + \mu_\delta(t - t_0) + \pi P_\delta + \Delta Y \quad . \tag{A4}$$

[5]The 5 standard parameters for HIP 50796 were actually computed as part of a 7-parameter solution incorporating the time derivatives of the proper motion components (since HIPPARCOS detected curvature in the proper motion). Nevertheless, the abscissae residuals available are always derived from the 5 standard parameters as listed in the catalog.

$P_\alpha$ and $P_\delta$ are the parallactic factors, and the terms $\Delta X = Bx + Gy$ and $\Delta Y = Ax + Fy$ represent the orbital motion components, where $A$, $B$, $F$, and $G$ are the classical Thiele-Innes constants. These depend only on the orbital elements $a_1$, $i$, $\omega_1$, and $\Omega$ (see, e.g., van de Kamp 1967). $x$ and $y$ are the rectangular coordinates in the unit orbit given by $x = \cos E - e$ and $y = \sqrt{1-e^2}\sin E$, with $E$ being the eccentric anomaly.

As described by Pourbaix & Jorissen (2000), the nature of the orbital solution is such that only the derivative corresponding to the semimajor axis in eq.(A2) needs to be considered. The expression for $\boldsymbol{\Xi}$ in eq.(A1) then reduces to

$$\boldsymbol{\Xi} = \boldsymbol{\Delta v} - \sum_{k=1}^{5} \frac{\partial \boldsymbol{v}}{\partial p_k}\Delta p_k - \left( \frac{\partial \boldsymbol{v}}{\partial \alpha_0^*}\Delta X + \frac{\partial \boldsymbol{v}}{\partial \delta_0}\Delta Y \right) \ . \tag{A5}$$

That the semimajor axis $a_1$ has actually been eliminated as a formal adjustable parameter in our case is irrelevant, since it still appears in the Thiele-Innes constant but is computed from other elements using eq.(1).

Finally, the $\chi^2$ for the global solution that combines astrometry and spectroscopy is computed by adding the term corresponding to the radial velocities, in the usual manner.

## REFERENCES

Baraffe, I., Chabrier, G., Allard, F., & Hauschildt, P. H. 1998, A&A, 337, 403

Bessell, M. S., & Brett, J. M. 1988, PASP, 100, 1134

Carpenter, J. M. 2001, AJ, 121, 2851

Chabrier, G., & Baraffe, I. 1997, A&A, 327, 1039

Chabrier, G., Baraffe, I., Allard, F., & Hauschildt, P. H. 2005, in Resolved Stellar Populations, ASP Conf. Ser., eds. D. Valls-Gabaud & M. Chavez, in press

Cox, A. N. 2000, Allen's Astrophysical Quantities, 4th Ed. (Berlin: Springer), 388

Delfosse, X., Forveille, T., Ségransan, D., Beuzit, J.-L., Udry, S., Perrier, C., & Mayor, M. 2000, A&A, 364, 217

ESA 1997, The Hipparcos and Tycho Catalogues, ESA SP-1200

Ferrario, L., Wickramasinghe, D., Liebert, J., & Williams, K. A. 2005, MNRAS, in press (see astro-ph/0506317)

Girardi, L., Bressan, A., Bertelli, G., & Chiosi, C. 2000, A&AS, 141, 371

Gizis, J. E. 2002, ApJ, 575, 484

Hemenway, P. D., Duncombe, R. L., Bozyan, E. P., Lalich, A. M., Argue, A. N., Franz, O. G., McArthur, B., Nelan, E., Taylor, D., White, G., Benedict, G. F., Crifo, F., Fredrick, L. W., Jefferys, W. H., Johnston, K., Kovalevsky, J., Kristian, J., Perryman, M. A. C., Preston, R., Shelus, P. J., Turon, C., & van Altena, W. 1997, AJ, 114, 2796

Henry, T. J., & McCarthy, D. W. 1993, AJ, 106, 773

Høg, E., Fabricius, C., Makarov, V. V., Urban, S., Corbin, T., Wycoff, G., Bastian, U., Schwekendiek, P., & Wicenec, A. 2000, A&A, 5355, L27

Jorissen, A., Jancart, S., & Pourbaix, D. 2004, in Spectroscopically and Spatially Resolving the Components of Close Binary Stars, ASP Conf. Ser. 318, eds. R. W. Hilditch, H. Hensberge and K. Pavlovski (San Francisco: ASP), 141

Kastner, J. H., Zuckerman, B., Weintraub, D. A., & Forveille, T. 1997, Science, 277, 67

Kurtz, M. J., & Mink, D. J. 1998, PASP, 110, 934

Latham, D. W. 1992, in IAU Coll. 135, Complementary Approaches to Double and Multiple Star Research, ASP Conf. Ser. 32, eds. H. A. McAlister & W. I. Hartkopf (San Francisco: ASP), 110

Latham, D. W., Nordström, B., Andersen, J., Torres, G., Stefanik, R. P., Thaller, M., & Bester, M. 1996, A&A, 314, 864

Latham, D. W., Stefanik, R. P., Torres, G., Davis, R. J., Mazeh, T., Carney, B. W., Laird, J. B., & Morse, J. A. 2002, AJ, 124, 1144

Makarov, V. V., & Fabricius, C. 2001, A&A, 368, 866

Micela, G., Favata, F., & Sciortino, S. 1997, A&A, 326, 221

Nordström, B., Latham, D. W., Morse, J. A., Milone, A. A. E., Kurucz, R. L., Andersen, J., & Stefanik, R. P. 1994, A&A, 287, 338

Pourbaix, D. 2004, in Spectroscopically and Spatially Resolving the Components of Close Binary Stars, ASP Conf. Ser. 318, eds. R. W. Hilditch, H. Hensberge and K. Pavlovski (San Francisco: ASP), 132

Pourbaix, D., Jancart, S., & Jorissen, A. 2004, in Spectroscopically and Spatially Resolving the Components of Close Binary Stars, ASP Conf. Ser. 318, eds. R. W. Hilditch, H. Hensberge and K. Pavlovski (San Francisco: ASP), 144

Pourbaix, D., & Jorissen, A. 2000, A&AS, 145, 161

Press, W. H., Teukolsky, S. A., Vetterling, W. T., & Flannery, B. P. 1992, Numerical Recipes, (2nd. ed.; Cambridge: Cambridge Univ. Press), 650

Song, I., Bessell, M. S., & Zuckerman, B. 2002, A&A, 385, 862

Song, I., Zuckerman, B., & Bessell, M. S. 2003, ApJ, 599, 342

Tachihara, K., Neuhäuser, R., Frink, S., & Guenther, E. 2003, Astron. Nachr., 324, 543

Torres, G., Guenther, E. W., Marschall, L. A., Neuhäuser, R., Latham, D. W., & Stefanik, R. P. 2003, AJ, 125, 825

Torres, G., Neuhäuser, R., & Latham, D. W. 2001, in Young Stars Near Earth: Progress and Prospects, ASP Conf. Ser. 244, eds. R. Jayawardhana & T. P. Greene, (San Francisco: ASP), 283

van de Kamp, P. 1967, Principles of Astrometry (San Francisco: W. H. Freeman), 141

van Leeuwen, F., & Evans, D. W. 1998, A&AS, 130, 157

Voges, W., Aschenbach, B., Boller, Th., Bräuninger, H., Briel, U., Burkert, W., Dennerl, K., Englhauser, J., Gruber, R., Haberl, F., Hartner, G., Hasinger, G., Kürster, M., Pfeffermann, E., Pietsch, W., Predehl, P., Rosso, C., Schmitt, J. H. M. M., Trümper, J., & Zimmermann, H. U. 1999, A&A, 349, 389

Zucker, S., & Mazeh, T. 1994, ApJ, 420, 806

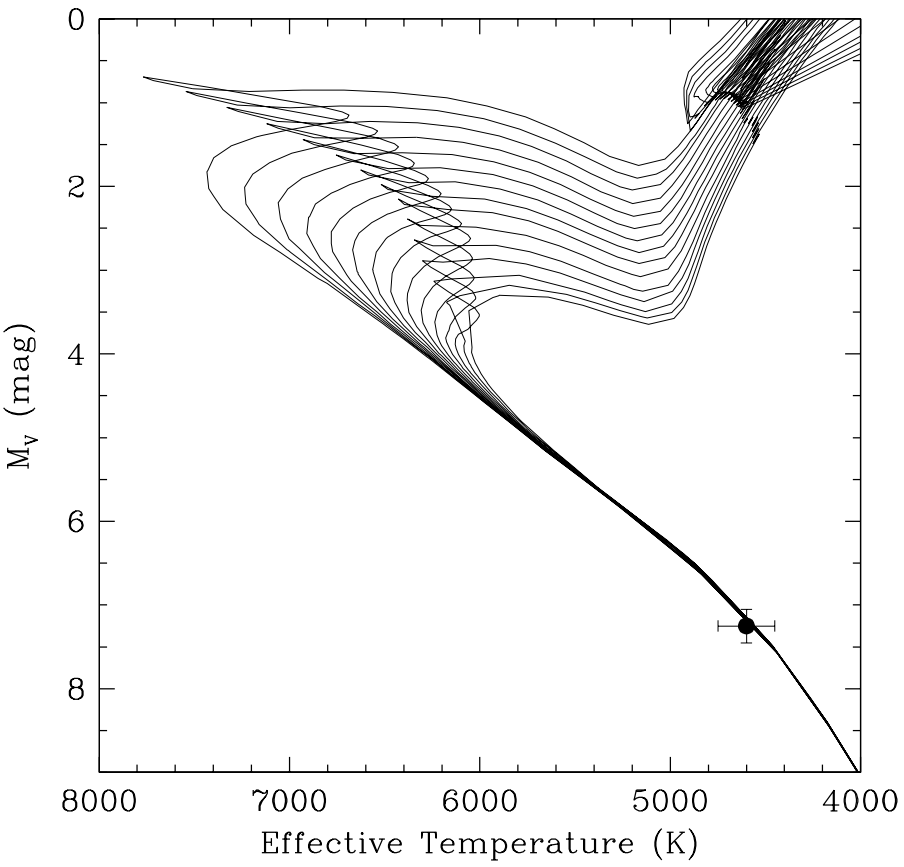


Fig. 1.— Location of HIP 50796 in the H-R diagram, against the backdrop of model isochrones by Girardi et al. (2000) for solar metallicity and ages ranging from 1 Gyr to 5 Gyr.

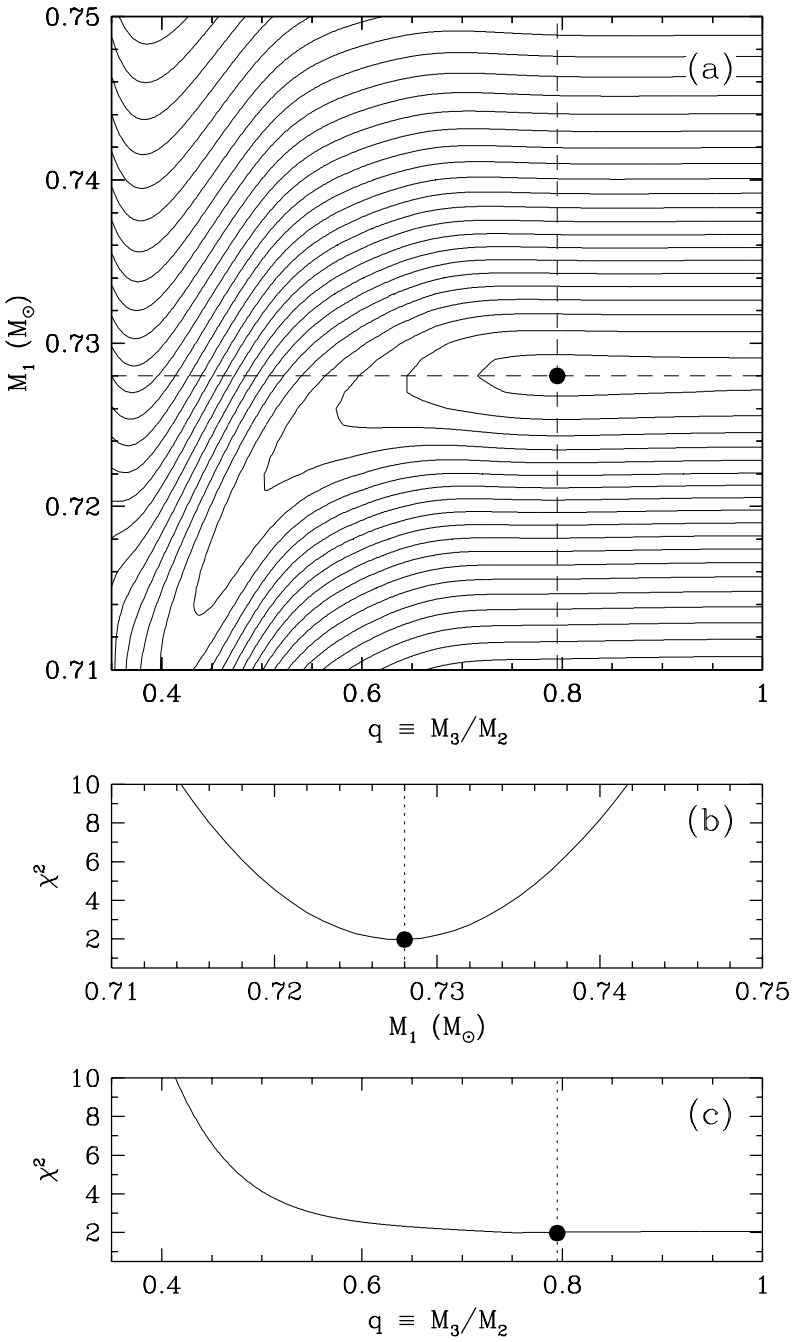


Fig. 2.— Morphology of the $\chi^2$ surface resulting from our modeling of the observed $V$ and $JHK$ photometry of HIP 50796 with the sum of three stars. (a) Contours of equal $\chi^2$. The dot represents the best fit with $M_1 = 0.728$ $M_\odot$ and a binary mass ratio of $q = 0.795$, corresponding to $M_2 = 0.49$ $M_\odot$ and $M_3 = 0.39$ $M_\odot$ (see text); (b) Cross-section along the $M_1$ axis, showing a well defined minimum; (c) Cross-section along the $q$ axis, showing a very flat $\chi^2$ surface in the vicinity of the minimum. Solutions at higher mass ratios and the same $M_1$ are not significantly worse.

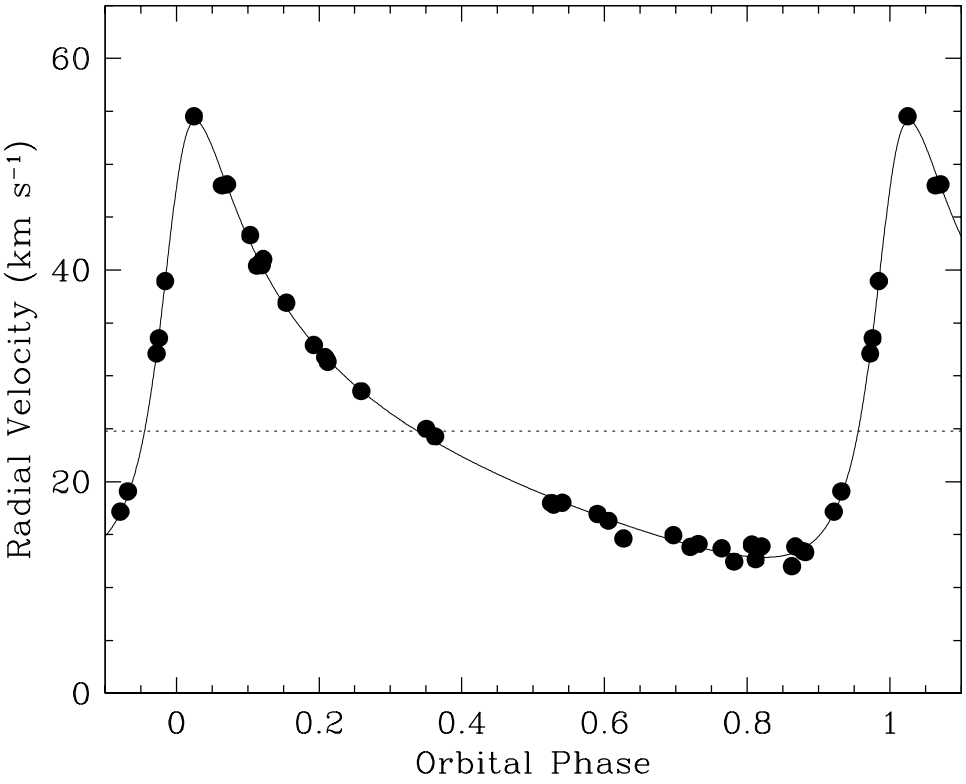


Fig. 3.— Radial velocity observations for HIP 50796 and fitted orbit. The dotted line represents the center-of-mass velocity of the binary. Errors are smaller than the size of the points.

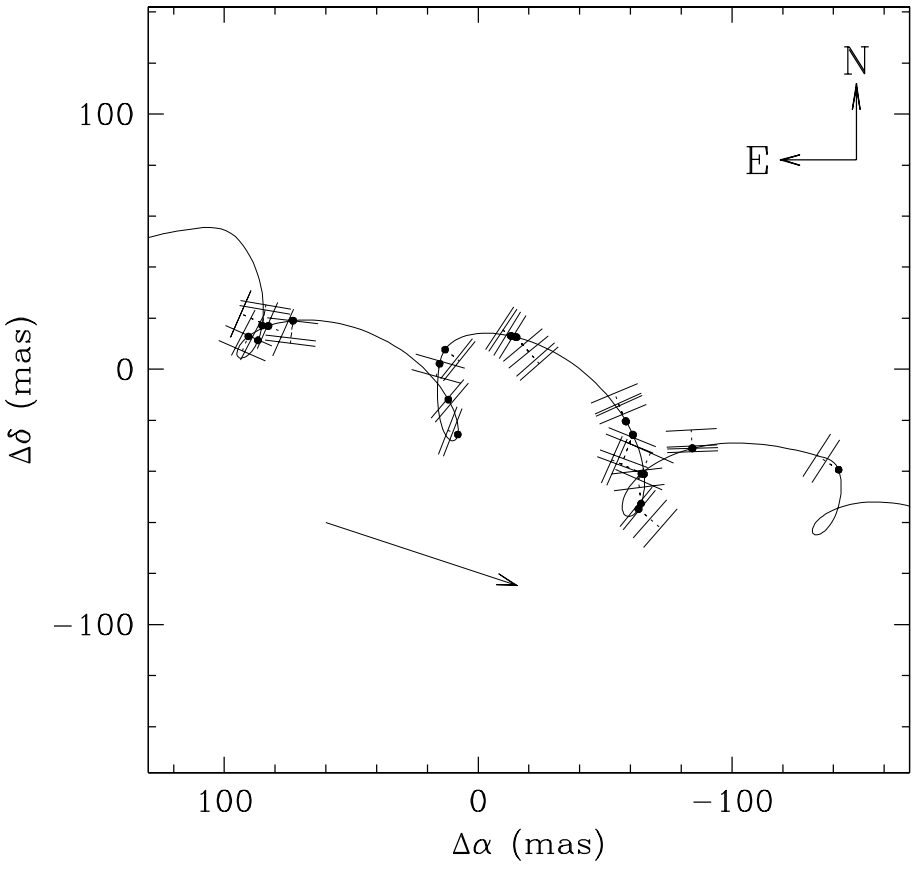


Fig. 4.— Path of the center of light of HIP 50796 on the plane of the sky, along with the HIPPARCOS observations (abscissae residuals). See text or Figure 5 for an explanation of the graphical representation of these one-dimensional measurements. The figure shows the total motion resulting from the combined effects of parallax, proper motion, and orbital motion according to the global solution described in the text. The arrow indicates the direction and magnitude of the annual proper motion.

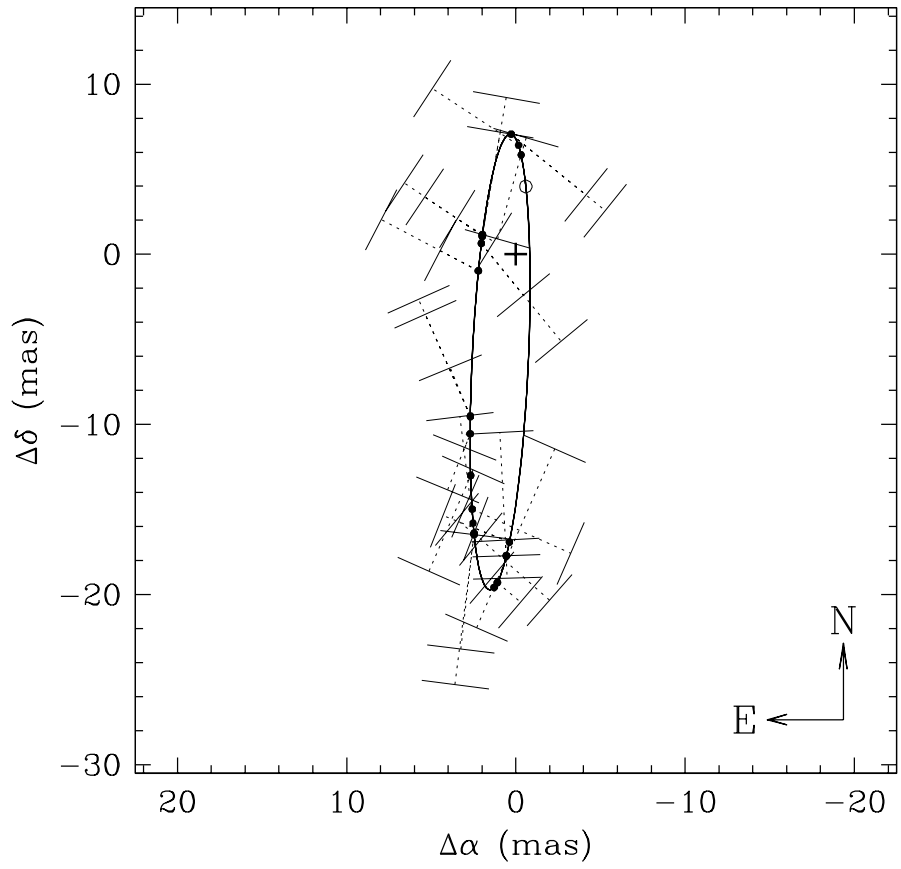


Fig. 5.— Residual orbital motion of the center of light of HIP 50796 on the plane of the sky, after removal of the parallactic and proper-motion components. HIPPARCOS observations are represented as in Figure 4 (a few measurements with large residuals have been omitted here for clarity). Because they are one-dimensional in nature (ESA 1997), the exact location of each measurement on the plane of the sky cannot be shown graphically. Filled circles represent the predicted location on the computed orbit. The dotted lines connecting to each filled circle indicate the scanning direction of the HIPPARCOS satellite for each measurement, and show which side of the orbit the residual is on. The short line segments at the end of and perpendicular to the dotted lines indicate the direction along which the actual observation lies, although the precise location is undetermined. Occasionally more than one measurement was taken along the same scanning direction, in which case two or more short line segments appear on the same dotted lines. The plus sign in the figure indicates the center of mass of the binary, and periastron is shown with an open circle. The direction of motion in the orbit is direct (counterclockwise).

Table 1. Radial velocity measurements for HIP 50796 in the heliocentric frame.

| HJD (2,400,000+) | Year | RV ($km\,s^{-1}$) | $\sigma_{RV}$[a] ($km\,s^{-1}$) | (O−C) ($km\,s^{-1}$) | Orbital Phase |
|---|---|---|---|---|---|
| 46422.9750 | 1985.9767 | +16.31 | 0.31 | −0.06 | 0.605 |
| 46537.6905 | 1986.2907 | +14.05 | 0.57 | +1.11 | 0.806 |
| 46540.7560 | 1986.2991 | +12.68 | 0.41 | −0.25 | 0.812 |
| 46569.7043 | 1986.3784 | +12.01 | 0.73 | −1.43 | 0.862 |
| 52391.6615 | 2002.3180 | +47.99 | 0.86 | −1.38 | 0.064 |
| 52395.7197 | 2002.3291 | +48.10 | 0.59 | +0.03 | 0.071 |
| 52419.6668 | 2002.3947 | +40.40 | 0.70 | −0.96 | 0.113 |
| 52421.6565 | 2002.4002 | +40.59 | 0.50 | −0.30 | 0.116 |
| 52423.6634 | 2002.4056 | +40.47 | 0.60 | +0.05 | 0.120 |
| 52424.6403 | 2002.4083 | +41.03 | 0.70 | +0.83 | 0.122 |
| 52655.0264 | 2003.0391 | +18.00 | 0.71 | −0.54 | 0.525 |
| 52656.9803 | 2003.0444 | +17.85 | 0.50 | −0.60 | 0.529 |
| 52663.9288 | 2003.0635 | +18.03 | 0.56 | −0.09 | 0.541 |
| 52691.9163 | 2003.1401 | +16.96 | 0.54 | +0.09 | 0.590 |
| 52712.8028 | 2003.1973 | +14.63 | 0.97 | −1.37 | 0.627 |
| 52752.7176 | 2003.3066 | +14.95 | 0.60 | +0.44 | 0.697 |
| 52772.7344 | 2003.3614 | +14.13 | 0.71 | +0.26 | 0.732 |
| 52985.0078 | 2003.9425 | +43.29 | 0.51 | +0.53 | 0.104 |
| 53013.9323 | 2004.0217 | +36.91 | 0.44 | +0.36 | 0.154 |
| 53035.8873 | 2004.0818 | +32.92 | 0.51 | −0.19 | 0.193 |
| 53044.9091 | 2004.1065 | +31.77 | 0.47 | −0.14 | 0.209 |
| 53046.9420 | 2004.1121 | +31.34 | 0.47 | −0.32 | 0.212 |
| 53073.7601 | 2004.1855 | +28.56 | 0.44 | −0.12 | 0.259 |
| 53125.7468 | 2004.3278 | +25.00 | 0.44 | +0.67 | 0.350 |
| 53132.7248 | 2004.3470 | +24.29 | 0.44 | +0.45 | 0.362 |
| 53337.0326 | 2004.9063 | +13.83 | 0.46 | −0.25 | 0.720 |
| 53362.0644 | 2004.9749 | +13.70 | 0.46 | +0.32 | 0.764 |
| 53371.9950 | 2005.0020 | +12.45 | 0.39 | −0.72 | 0.782 |
| 53393.8773 | 2005.0620 | +13.90 | 0.39 | +0.97 | 0.820 |
| 53420.9096 | 2005.1360 | +13.88 | 1.13 | +0.47 | 0.867 |
| 53426.8509 | 2005.1522 | +13.46 | 0.51 | −0.27 | 0.878 |
| 53428.8623 | 2005.1577 | +13.35 | 0.51 | −0.52 | 0.881 |
| 53451.7621 | 2005.2204 | +17.17 | 0.36 | +0.11 | 0.921 |
| 53457.7802 | 2005.2369 | +19.09 | 0.50 | +0.37 | 0.932 |
| 53480.8179 | 2005.3000 | +32.11 | 0.41 | +0.03 | 0.972 |
| 53482.6947 | 2005.3051 | +33.57 | 0.44 | −0.26 | 0.976 |
| 53487.7003 | 2005.3188 | +38.96 | 0.44 | +0.07 | 0.984 |
| 53510.6947 | 2005.3818 | +54.52 | 0.43 | +0.13 | 0.025 |

[a]Velocity uncertainties include the scale factor described in the text.

Table 2. Orbital solutions for HIP 50796.

| Parameter | Spectroscopic only | Combined[a] | Constrained[a,b] |
|---|---|---|---|
| Adjusted quantities | | | |
| $P$ (days) | 570.70 ± 0.73 | 570.95 ± 0.52 | 570.98 ± 0.52 |
| $\gamma$ (km s$^{-1}$) | +24.77 ± 0.14 | +24.86 ± 0.11 | +24.87 ± 0.11 |
| $K$ (km s$^{-1}$) | 20.62 ± 0.28 | 20.75 ± 0.20 | 20.76 ± 0.20 |
| $e$ | 0.6103 ± 0.0071 | 0.6110 ± 0.0052 | 0.6110 ± 0.0051 |
| $\omega_1$ (deg) | 313.75 ± 0.95 | 314.01 ± 0.76 | 314.02 ± 0.76 |
| $T$ (HJD−2,400,000) | 52355.2 ± 1.4 | 52355.0 ± 1.1 | 52355.0 ± 1.1 |
| $i$ (deg) | ··· | 85 ± 13 | 83 ± 15 |
| $\Omega$ (deg) | ··· | 175.0 ± 8.8 | 179 ± 10 |
| $\Delta\alpha^*$ (mas) | ··· | +3.7 ± 4.0 | +3.1 ± 4.2 |
| $\Delta\delta$ (mas) | ··· | −8.7 ± 1.8 | −7.7 ± 1.7 |
| $\Delta\mu^*_\alpha$ (mas yr$^{-1}$) | ··· | +4.6 ± 1.4 | +4.5 ± 1.4 |
| $\Delta\mu_\delta$ (mas yr$^{-1}$) | ··· | −3.4 ± 1.3 | −3.2 ± 1.3 |
| $\Delta\pi$ (mas) | ··· | −9.9 ± 1.8 | −8.8 ± 1.9 |
| Derived quantities | | | |
| $f(M)$ ($M_\odot$) | 0.258 ± 0.011 | ··· | ··· |
| $M_2 \sin i/(M_1+M_2)^{2/3}$ ($M_\odot$) | 0.6364 ± 0.0092 | ··· | ··· |
| $a_1 \sin i$ ($10^6$ km) | 128.2 ± 1.9 | ··· | ··· |
| $a_1$ (mas) | ··· | 16.9 ± 1.5 | 17.9 ± 1.6 |
| $a_{\rm phot}$ (mas) | ··· | 16.9 ± 1.5 | 14.9 ± 1.3 [c] |
| $a$ (AU)[c] | ··· | 1.580 ± 0.029 | 1.582 ± 0.032 |
| $a$ (mas)[c] | ··· | 30.8 ± 3.2 | 32.5 ± 3.3 |
| $\mu^*_\alpha$ (mas yr$^{-1}$) | ··· | −75.4 ± 1.4 | −75.5 ± 1.4 |
| $\mu_\delta$ (mas yr$^{-1}$) | ··· | −25.0 ± 1.3 | −24.8 ± 1.3 |
| $\pi$ (mas) | ··· | 19.5 ± 1.8 | 20.6 ± 1.9 |

[a]Incorporates radial velocities, HIPPARCOS measurements (abscissae residuals), and the Tycho-2 proper motions.

[b]Assumes the light from the secondary is not negligible (a brightness difference of $\Delta V = 2.5$ mag); see text.

[c]Assumes a value for the primary mass of $M_1 = 0.73$ $M_\odot$.

Table 3. HIPPARCOS abscissae residuals for HIP 50796.

| HJD (2,400,000+) | Year | $v$ (mas) | $\sigma_v$ (mas) | Cons.[a] | Corr. Coef.[b] | $O-C$ (mas) | Orbital Phase |
|---|---|---|---|---|---|---|---|
| 47884.3184 | 1989.9776 | −6.60 | 4.60 | F | 0.762 | −5.24 | 0.170 |
| 47884.1723 | 1989.9772 | −8.65 | 5.40 | N | 0.762 | −7.30 | 0.170 |
| 47901.6313 | 1990.0250 | +1.61 | 5.67 | F | 0.531 | −6.77 | 0.200 |
| 47901.5947 | 1990.0249 | +5.55 | 4.55 | N | 0.531 | −2.84 | 0.200 |
| 48020.3010 | 1990.3499 | +3.81 | 4.31 | F | 0.736 | +0.01 | 0.408 |
| 48020.1914 | 1990.3496 | −2.70 | 5.51 | N | 0.736 | −6.49 | 0.408 |
| 48046.1241 | 1990.4206 | +20.01 | 8.67 | F | 0.868 | +12.78 | 0.453 |
| 48046.0146 | 1990.4203 | +20.01 | 10.75 | N | 0.868 | +12.78 | 0.453 |
| 48046.3068 | 1990.4211 | +1.86 | 4.72 | F | 0.773 | −5.37 | 0.454 |
| 48046.3798 | 1990.4213 | +8.67 | 5.82 | N | 0.773 | +1.44 | 0.454 |
| 48069.0619 | 1990.4834 | +6.63 | 8.84 | F | 0.878 | +0.25 | 0.494 |
| 48069.0619 | 1990.4834 | −0.14 | 9.83 | N | 0.878 | −6.53 | 0.494 |
| 48069.2445 | 1990.4839 | −2.29 | 6.59 | F | 0.000 | −8.62 | 0.494 |
| 48203.1086 | 1990.8504 | −1.80 | 3.97 | F | 0.789 | +2.00 | 0.728 |
| 48203.0721 | 1990.8503 | −4.01 | 4.66 | N | 0.789 | −0.22 | 0.728 |
| 48249.2397 | 1990.9767 | −3.38 | 11.29 | F | 0.950 | −3.45 | 0.809 |
| 48249.2397 | 1990.9767 | −1.29 | 12.87 | N | 0.950 | −1.37 | 0.809 |
| 48367.3615 | 1991.3001 | −17.97 | 5.69 | F | 0.798 | −1.14 | 0.016 |
| 48367.2520 | 1991.2998 | −24.12 | 7.29 | N | 0.798 | −7.32 | 0.016 |
| 48383.7978 | 1991.3451 | −7.19 | 6.53 | F | 0.853 | −5.25 | 0.045 |
| 48383.7978 | 1991.3451 | −8.67 | 7.31 | N | 0.853 | −6.71 | 0.045 |
| 48454.3275 | 1991.5382 | −1.37 | 6.17 | F | 0.853 | −0.54 | 0.168 |
| 48454.2910 | 1991.5381 | +1.18 | 7.44 | N | 0.853 | +2.00 | 0.168 |
| 48454.8024 | 1991.5395 | +4.31 | 3.93 | F | 0.768 | +5.72 | 0.169 |
| 48454.7658 | 1991.5394 | +2.88 | 4.82 | N | 0.768 | +4.26 | 0.169 |
| 48458.3088 | 1991.5491 | −17.61 | 4.83 | F | 0.825 | −12.14 | 0.175 |
| 48458.3453 | 1991.5492 | −19.79 | 5.64 | N | 0.825 | −14.34 | 0.175 |
| 48458.7471 | 1991.5503 | −10.35 | 4.28 | F | 0.753 | −4.42 | 0.176 |
| 48458.7471 | 1991.5503 | −13.81 | 4.59 | N | 0.753 | −7.92 | 0.176 |
| 48551.9954 | 1991.8056 | −6.38 | 5.31 | F | 0.799 | −7.26 | 0.339 |
| 48551.9223 | 1991.8054 | −5.40 | 5.89 | N | 0.799 | −6.29 | 0.339 |
| 48552.2145 | 1991.8062 | −2.14 | 6.75 | F | 0.683 | −2.89 | 0.340 |
| 48552.3606 | 1991.8066 | −11.07 | 10.06 | N | 0.683 | −11.80 | 0.340 |
| 48562.6972 | 1991.8349 | +5.40 | 6.78 | F | 0.779 | +9.22 | 0.358 |
| 48562.5146 | 1991.8344 | +8.30 | 9.05 | N | 0.779 | +12.09 | 0.358 |
| 48562.9164 | 1991.8355 | −1.35 | 5.10 | F | 0.730 | +2.59 | 0.358 |
| 48562.9894 | 1991.8357 | −4.05 | 6.93 | N | 0.730 | −0.10 | 0.359 |
| 48595.8984 | 1991.9258 | −9.20 | 9.97 | F | 0.894 | −10.50 | 0.416 |
| 48595.7889 | 1991.9255 | −11.43 | 11.07 | N | 0.894 | −12.75 | 0.416 |
| 48629.5380 | 1992.0179 | −17.27 | 4.36 | F | 0.778 | −7.63 | 0.475 |
| 48629.7206 | 1992.0184 | −23.85 | 4.97 | N | 0.778 | −14.20 | 0.475 |
| 48638.9614 | 1992.0437 | +5.21 | 4.58 | F | 0.735 | +11.59 | 0.492 |
| 48638.8519 | 1992.0434 | −0.26 | 4.85 | N | 0.735 | +6.12 | 0.491 |
| 48639.2901 | 1992.0446 | −5.36 | 4.10 | F | 0.686 | +0.77 | 0.492 |
| 48639.3632 | 1992.0448 | −7.20 | 4.02 | N | 0.686 | −1.06 | 0.492 |

Table 3—Continued

| HJD (2,400,000+) | Year | $v$ (mas) | $\sigma_v$ (mas) | Cons.[a] | Corr. Coef.[b] | $O-C$ (mas) | Orbital Phase |
|---|---|---|---|---|---|---|---|
| 48760.4436 | 1992.3763 | +9.38 | 9.65 | F | 0.751 | +10.30 | 0.704 |
| 48760.4070 | 1992.3762 | −2.08 | 13.41 | N | 0.751 | −1.18 | 0.704 |
| 48808.2183 | 1992.5071 | +10.67 | 11.83 | F | 0.875 | +8.18 | 0.788 |
| 48809.0218 | 1992.5093 | +4.26 | 13.06 | N | 0.875 | +1.84 | 0.789 |
| 48809.2410 | 1992.5099 | +3.03 | 5.48 | F | 0.505 | +0.89 | 0.790 |
| 48809.0949 | 1992.5095 | +1.71 | 9.46 | N | 0.505 | −0.42 | 0.790 |
| 48942.7033 | 1992.8753 | −2.01 | 6.43 | F | 0.777 | −9.08 | 0.024 |
| 48942.7033 | 1992.8753 | +2.19 | 7.92 | N | 0.777 | −4.88 | 0.024 |

[a]Data reduction consortium responsible for the measurement: F = FAST, N = NDAC (see ESA 1997).

[b]Correlation coefficient between the FAST and NDAC abscissae taken on the same great circle.

Table 4. Parallax and proper motion components of HIP 50796.

| Source | $\mu^*_\alpha$ (mas yr$^{-1}$) | $\mu_\delta$ (mas yr$^{-1}$) | $\pi$ (mas) |
|---|---|---|---|
| HIPPARCOS catalog (ESA 1997) ... | $-80.0 \pm 2.4$ | $-21.6 \pm 1.9$ | $29.4 \pm 2.7$ |
| Initial fit (this paper)[a] ..... | $-76.1 \pm 2.2$ | $-24.6 \pm 1.8$ | $19.4 \pm 1.9$ |
| Tycho-2 catalog (Høg et al. 2000) ... | $-74.9 \pm 1.8$ | $-25.3 \pm 1.8$ | ··· |
| Combined fit (this paper)[b] ..... | $-75.4 \pm 1.4$ | $-25.0 \pm 1.3$ | $19.5 \pm 1.8$ |
| Constrained fit (this paper)[c] ..... | $-75.5 \pm 1.4$ | $-24.8 \pm 1.3$ | $20.6 \pm 1.9$ |

[a]Incorporates radial velocities and HIPPARCOS abscissae residuals, but not the Tycho-2 proper motions.

[b]Includes the Tycho-2 proper motions, and assumes the companion contributes no light.

[c]Accounts for the small light contribution from the companion.

Table 5. Photometry for HIP 50796.

| Source | $M_V$ (mag) | $V-J$ (mag) | $V-H$ (mag) | $V-K$ (mag) |
|---|---|---|---|---|
| Observed ($\pi$ from combined solution) ..... | 7.25 ± 0.20 | 2.32 ± 0.03 | 2.99 ± 0.04 | 3.10 ± 0.04 |
| Girardi et al. (2000) isochrones[a] ..... | 7.25 | 1.96 | 2.60 | 2.67 |
| Henry & McCarthy (1993)[a] ..... | 7.22 | 2.15 | 2.70 | 2.85 |
| Observed ($\pi$ from constrained solution) ... | 7.37 ± 0.20 | 2.32 ± 0.03 | 2.99 ± 0.04 | 3.10 ± 0.04 |
| Model for triple system ..... | 7.14 | 2.34 | 2.95 | 3.12 |

[a]Predicted photometry for a single star with $M_1 = 0.73$ $M_\odot$.